Reduction of Sidelobes by Nonuniform Elements Spacing of a Spherical Antenna Array

Slavko RUPCIC, Vanja MANDRIC, Drago ZAGAR

J. J. Strossmayer University of Osijek, Kneza Trpimira 2b, 31000 Osijek, Croatia

rupcic@etfos.hr, vmandric@etfos.hr, drago.zagar@etfos.hr

Abstract. *This paper presents a significant sidelobe reduction if nonuniform elevational spacing of antenna elements on the sphere is used. Antenna elements are progressively phased with a uniform amplitude excitation. The calculation of the required element position is presented. The achieved sidelobe level reduction with unequally spaced arrays could reach even more than 20dB difference with regard to the first significant sidelobe level of equally spaced arrays. By this method, arrays have the ability to produce the desired radiation pattern and could satisfy requirements for many applications.*

Keywords

Radiation pattern, spherical array, sidelobe level reduction, uniform and nonuniform distribution of antenna elements.

1. Introduction

Since the 1990s, there has been enormous interest in multiantenna systems. As spectrum became a more and more precious resource, researchers investigated ways of improving the capacity of wireless systems without actually increasing the required spectrum. Multiantenna systems offer such a possibility [1].

Smart antenna arrays can provide an efficient way to increase the data rate in the future of wireless systems. Smart antennas work by the principle of combining antenna array with signal processing to optimize automatically the beam pattern in response to the received signal. Array antennas have capability of fast electronic beam steering. Also, they can be designed to offer reconfigurability, conformal characteristics, multi beam capabilities and adaptive pattern reshaping. Recently, there has been a growing interest in designing spherical antenna arrays.

The present study was undertaken to evaluate the possible merits of a spherical phased-array with nonuniformly spaced antenna elements in providing directive pattern with sidelobes below those for uniform arrays and complete hemispherical coverage without appreciable loss of gain. For spherical array, an active sector can be moved along surface and the scan angle is increased. The grating lobe phenomenon is reduced by using nonuniform antenna elements spacing.

The use of arbitrary element position for pattern synthesis purposes was suggested by Unz [2]. King, Packard and Thomas [3] proposed the use of unequal spacing in a linear array to reduce grating lobes and computed the pattern of various trial sets. Sandler [4] expanded a term for each element in series. Harrington [5] presented a method for reducing sidelobe levels of linear array by using nonuniform element spacing, while retaining uniform excitation. It is shown that the side-lobes can be reduced in height to approximately $2/N$ times the main lobe level, where N is the number of antenna elements. Andreasen [6] computed the various possibilities of unequally-spaced arrays (linear). Ishimaru [7] presented new approach to the unequally-spaced array problem. It is based on the use of Poisson's sum formula and the introduction of a new function, the "source position function". By this method, it is possible to design unequally-spaced arrays which produce a desired radiation pattern. In the paper of Hodjat and Hovanessian [8], an iteration method based on the solution of a set of linear simultaneous equation at each iteration is proposed for calculating the distance between the elements of a symmetrical nonuniformly spaced linear array antenna for sidelobe reduction. In the second part of the paper, several symmetrical nonuniformly spaced planar array antennas have been designed, using the nonuniform linear array spacing. Jarske [9] showed that the element spacings of the optimal solution are integer multiplies of a suitable chosen basic spacing and presented two design procedures for nonuniformly spaced linear arrays. Pozar and Kaufman discussed and quantified the factors affecting the realizable sidelobe performance of mirostrip arrays [10]. For the unequally spaced arrays, Jeffers presented the successive approximation method and dynamic program method [11]. Kummar and Branner presented an analytical technique for synthesis of unequally spaced arrays with linear, planar, cylindrical and spherical geometry [12]. Shihab designed a non-uniform circular antenna array using particle swarm optimization [13]. Abdolee developed a simple and fast genetic algorithm to reduce the sidelobe in non-uniformly spaced linear arrays [14]. Bevelacqua and Balanis determined optimal array geometries using the Particle Swarm Optimization (PSO) algorithm with optimal weights in order to minimize sidelobe levels in wideband arrays [15].

The effect of unequal spacing in spherical arrays has been studied by computing the radiation pattern for a specific element arrangement at a given frequency and with the beam steered in a given direction.

The following characteristics were chosen as goals for the investigation reported herein:

- array to have a single narrow main beam;
- array to have all sidelobes below the main beam level;
- nonuniform arrays to have sidelobe levels below uniform sidelobe level;
- $HPWB_{uni}/HPWB_{nonuni}$ ratio to have maximum 1.8;
- array elements to have minimum spacing of the antenna element diameter.

Excitation of antenna elements is constant and uniform and elements are progressively phased. Minimum element spacing is equal to the antenna element diameter (waveguide diameter).

This paper presents the reduction of sidelobe levels by using nonuniform element spacing on the spherical surface.

2. Far Field Calculation of Spherical Arrays

Arrays like the previously mentioned array are conformal antennas and periodic structures. They are frequently analyzed by means of the electric field integral equation and the moment method. The kernel of the integral operator is Green's function, which could be different for different structures.

In this paper, we deal with one-dimensional spherical structures (the spherical structure varies in radial direction and is homogeneous in θ and φ directions) that can be analyzed using spectral domain approach. Since the considered problem is defined in the spherical coordinate system, the vector-Legendre transformation [16], [17] is applied.

$$\mathbf{M}(r,\theta,\phi)=\sum_{m=-\infty}^{\infty}\sum_{n=|m|}^{\infty}\widetilde{\mathbf{L}}(n,m,\theta)\widetilde{\mathbf{M}}(r,n,m)e^{jm\phi}\,, \tag{1}$$

$$\widetilde{\mathbf{M}}(r,n,m)=\frac{1}{2\pi S(n,m)}\cdot$$

$$\int_{-\pi}^{\pi}\int_{0}^{\pi}\widetilde{\mathbf{L}}(n,m,\theta)\mathbf{M}(r,\theta,\phi)\sin\theta e^{-jm\phi}d\theta d\phi\,, \tag{2}$$

$$\widetilde{\mathbf{L}}(n,m,\theta)=$$

$$\begin{bmatrix} P_n^{|m|}(\cos\theta)\sqrt{n(n-1)} & 0 & 0 \\ 0 & \dfrac{\partial P_n^{|m|}(\cos\theta)}{\partial\theta} & \dfrac{-jmP_n^{|m|}(\cos\theta)}{\sin\theta} \\ 0 & \dfrac{jmP_n^{|m|}(\cos\theta)}{\sin\theta} & \dfrac{\partial P_n^{|m|}(\cos\theta)}{\partial\theta} \end{bmatrix} \tag{3}$$

$$S(n,m)=\frac{2n(n-1)(n+|m|)!}{(2n+1)(n-|m|)!} \tag{4}$$

Here n, m are variables in the spectral domain, $\widetilde{\mathbf{L}}(n,m,\theta)$ is the kernel of the vector–Legendre transformation, $\widetilde{\mathbf{M}}(r,n,m)$ is a spectral domain equivalent magnetic current placed at the open of each waveguide and $P_n^{|m|}(\cos\theta)$ are the associated Legendre functions of the first kind.

The electric field radiated by the current shell on the spherical surface in homogeneous media is:

$$\mathbf{E}(r,\theta,\phi)=\sum_{m=-\infty}^{\infty}\sum_{n=|m|}^{\infty}\overline{\overline{\mathbf{L}}}(n,m,\theta)\widetilde{\overline{\overline{\mathbf{G}}}}(n,m,r|r_s)\widetilde{\mathbf{M}}(r,n,m)e^{jm\phi} \tag{5}$$

where $\widetilde{\overline{\overline{\mathbf{G}}}}(n,m,r|r_s)$ is the spectral domain dyadic Green's function for a grounded spherical surface.

The appropriate spectral – domain Green's function of a multilayer one-dimensional spherical structure is calculated using the G1DMULT algorithm [19].

Calculation of the far field radiation patterns of a spherical array is explained in [18], [19] and [20].

The complete pattern expression of the field produced by the array is given as ([18], [20]):

$$E(\theta,\phi)=\sum_{k,l}E_{\alpha_l\beta_{lk}}(\theta,\phi)\,. \tag{6}$$

3. Uniformly Spaced Antenna Element

If we want to get more directional beam pattern we must use an antenna array. Antenna arrays are usually thought of as having equal spacing between antenna elements but this is not necessary. Also, since our purpose is to investigate unequally spaced arrays, it is instructive to see radiation pattern of uniform spaced arrays and use it as a referent pattern.

We used icosahedral structure to provide uniform distribution of antenna elements. Icosahedron is a three-dimensional geometrical element which consists of twenty equal equilateral triangles. Icosahedron has 30 edges and 20 vertices. The icosahedron type of element arrangement that is used in the spherical array is given by [19]

$$\alpha_{l0}=A_0+B_0\cdot l, \tag{7}$$

where A_0 = 90°, B_0 = -15, l is an integer in range $-6 \le l \le 6$, and

$$\beta_{lk}=\frac{72°k}{6-|l|}\text{, for } l = 5, 4, 3, 2; \tag{8}$$

$$\beta_{lk}=180°+\frac{72°k}{6-|l|}\text{, for } l = -5, -4, -3, -2; \tag{9}$$

$$\beta_{\pm 6k}=0\,,\ \beta_{\pm 1k}=\beta_{2k}+9°\ \text{and}\ \beta_{0k}=\beta_{2k}\,, \tag{10}$$

where k is a positive integer ranging from 0 to a value $M(l)$ which depends on l. With the expressions (7) to (10) the values of $M(l)$ may be obtained as follows:

$$M(l) = 5(6-|l|)-1\text{, for } l = \pm5, \pm4, \pm3, \pm2; \tag{11}$$

$$M(6) =0,\ M(0) = M(1) = M(2). \tag{12}$$

If the elements are arranged in this way there are 162 elements placed over the entire spherical surface ($-6 \le l \le 6$). For a hemispherical surface ($0 \le l \le 6$) the total number of antenna elements used is 91.

With the element distribution given by (7) to (12), the number of antenna elements used for different values α is given in Tab. 1 when $\theta_0 = 0$ and $\varphi_0 = 0$.

l	α_{l0}	Number of antennas on l-th ring	Total number of antennas
0	90°	20	91
1	75°	20	71
2	60°	20	51
3	45°	15	31
4	30°	10	16
5	15°	5	6
6	0°	1	1

Tab. 1. Number of antenna elements used for a hemispherical surface ($0 \le n \le 6$).

Fig. 1 shows geometrical (icosahedronical) representation of the antenna element distribution on the spherical surface.

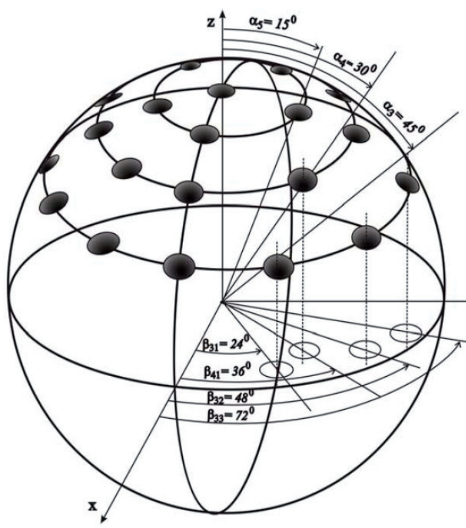

Fig. 1. Geometrical representation of the uniform antenna element distribution on the spherical surface [5].

4. Nonuniformly Spaced Antenna Elements

The main advantage of nonuniformly spaced arrays presented in this paper is the reduction of sidelobe levels by using nonuniform elements spacing, while retaining uniform excitation. Nonuniform spacing of elements means that icosahedronical structure mentioned in the previous section is perturbed.

It is possible to achieve nonuniform antenna elements spacing on the spherical surface by changing elevational, azimuthal or both position angles. However, when we set the direction of the main beam (maximum of radiation) defined by angles θ_0 and φ_0 on the north pole of the spherical surface, then we have only one option to achieve a useful nonuniform antenna spacing. In that case we are able to change only the elevational angle (α_l - see Fig. 1) position of the antenna elements. Moving azimuthal angle (β_{lk}) of the antenna elements leads significantly to unwanted degradation of E and H radiation pattern, as well as to change of the main beam direction (the radiation pattern becomes asymmetric).

The change of the main lobe direction out of the pole of the sphere requires changes of elevational and azimuthal position of the antenna elements, which are subset of the array that radiates in the defined direction.

If we want to properly analyze the influence of change in distance of antenna elements on the sphere due to different functions of the distance of antenna elements, it is satisfactory to present the example of maximum radiation in the direction of the north pole of the sphere.

To reach the main goal of these antenna arrays – low sidelobes, the appropriate function of the antenna elements positions must be found. The minimal distance between antenna elements was limited by physical dimension of the used antenna elements. In our case, the antenna elements are circular waveguides with 12 cm diameter which is the minimal possible distance between antenna elements.

Furthermore, based on uniform spaced arrays it is known that arrays with high space density have higher main beam-sidelobe level distance. Therefore, we have decided to increase space density near the direction of maximum radiation (first rings) and decrease space density far from the direction of maximum radiation (last rings). That was the reason for using convex function of the antenna element spacing (or convex functions segments).

Five array configurations of unequally-spaced elements have been chosen on the basis of which antenna elements are sorted and basic idea of research is realized.

4.1 Exponential Spacing Scheme

The first convex function (spacing scheme) to be mentioned is the exponential one and is expressed with

$$\alpha_{l1} = A_1 + B_1 \cdot e^{\left(\frac{l}{C_1}\right)} \tag{13}$$

where α_{l1} presents elevational angles (alpha) which are comprised with the above mentioned expression, l are the circles with antenna elements where β_{lk} determines the location of each element. The smallest spacing ($\alpha_{min} = 6.55^0$) is next to the north pole of the sphere and it is determined as a minimal possible distance between antenna elements. The elevation angles are shown in Tab. 2.

4.2 Polynomial Spacing Scheme

The second convex function is polynomial function

$$\alpha_{l2} = A_2 + B_2 \cdot l + C_2 \cdot l^2 + D_2 \cdot l^3 \tag{14}$$

where α_{l2} and l have the same meaning as in the previous equations. Elevation angles of rings for this case are very similar to the angles in the previous (exponential) case and we expect similar effect on radiation pattern. The total number of the used rings (also the total number of antenna elements) is the same for uniform and all five nonuniform spacing schemes. Elevation angles for the polynomial spacing scheme are shown in Tab. 2.

NONUNIFORM SPACING SCHEME	α_{5i} (deg)	α_{4i} (deg)	α_{3i} (deg)	α_{2i} (deg)	α_{1i} (deg)
Exponential (i = 1)	6.58	13.98	22.31	31.66	42.18
Polynomial (i = 2)	6.55	13.99	22.51	32.24	43.35
Trigonometric (i = 3)	6.57	15.73	26.59	38.10	49.15
Logarithmic (i = 4)	6.55	14.39	24.11	36.97	55.99
Prime number (i = 5)	6.94	14.67	22.66	31.44	40.74

Tab. 2. Elevation angles of different spacing schemes of the circular waveguide-fed aperture arrays on a spherical surface.

4.3 Trigonometrical (Cosine) Spacing Scheme

Another elevational distribution of the circular rings on spherical surface which could be used to reduce side-lobe levels of the radiation pattern is a trigonometrical function. The trigonometrical function is given with

$$\alpha_{l3} = A_3 + B_3 \cdot \cos\left(\frac{l}{C_3} - D_3\right) \tag{15}$$

α_{13} also presents elevational angles (alpha) which are comprised with the above expression, and l are numbers of circles with antenna elements. Elevation angles for the trigonometrical spacing scheme are shown in Tab. 2.

4.4 Logarithmic Spacing Scheme

The waveguide antenna elements are placed on elevational rings of a spherical surface at numerical intervals over one logarithmic cycle. The smallest spacing is next to the north pole of the sphere and the distance of the l-th element from the pole is

$$\alpha_{l4} = A_4 + B_4 \cdot \log(l + C_4) \tag{16}$$

This spacing scheme has maximal value of the last elevation angles (α_{14} = 55.99^0). Elevation angles for the logarithmic spacing scheme are shown in Tab. 2.

4.5 Prime Number Spacing Scheme

Another attempt to choose spacing was to derive a set of spacing from a sequence of prime numbers [3]. The prime number spacing scheme cannot be described by the function. Prime number procedure is illustrated by the data in Tab. 3. The ring angle α_{l5} was determined as a product of the minimal element distance and the distance defined by the chosen prime number sequence (column Distance in Tab. 3).

5. Numerical Results

Situations with uniformly spaced elements and all five examples of unequally spaced antenna elements have constant basic parameters. Basic structure is icosahedronical which is perturbed in other cases.

Ring number l	Prime number PN	2xPN/100	Distance	Ring angle α_{l5} (deg)
5	53	1.06	1.06	6.94
4	59	1.18	2.24	14.67
3	61	1.22	3.46	22.66
2	67	1.34	4.80	31.44
1	71	1.42	6.22	40.74

Tab. 3. Elevation angles of the prime number spacing scheme of the circular waveguide-fed aperture array on a spherical surface.

The hemispherical arrays (uniform and nonuniform) under consideration have the following properties>

- array elements are composed of circular waveguide fed apertures;
- the number of elevation rings in arrays is 5 and one antenna element is located at the north pole;
- initial uniform spacing of elevation rings in array leading icosahedronical distribution;
- the number of equally spaced elements in every ring leading icosahedronical distribution (Tab. 1.) (for uniform and nonuniform spacing schemes);
- the total number of antenna elements in arrays is 71;
- the radius of the spherical surface r_s is 65.5 cm (3.83λ);
- the radius of the circular waveguide-fed aperture r_w is 6 cm (0.35λ);
- the working frequency is f = 1.75 GHz.

All antenna elements are constantly and equally excited, and progressively phased.

5.1 Uniformly Spaced Antenna Elements

When antenna elements are equally spaced (α_l = 0°, 15°, 30°, 45°, 60°, 75°) the value of the first significant sidelobe is -9.55 dB down from the main lobe level for E – plane and -12.66 dB down from the main lobe level for H – plane. These levels are the reference levels for comparing other spacing schemes. Notice, the first significant sidelobe level is the highest backside lobe level. Fig. 2. shows the radiation pattern of the uniformly distributed antenna elements placed on the sphere for E – plane and H - plane.

More desirable for many directive applications is the lower sidelobe level.

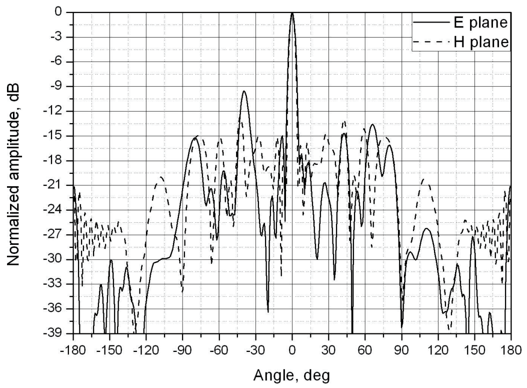

Fig. 2. Radiation pattern of uniformly distributed antenna elements placed on the sphere (E-plane and H-plane).

5.2 Nonuniformly Spaced Antenna Elements

5.2.1 Antenna Elements Comprised by the Exponential Function

It is obvious that when this kind of nonuniformly spaced antenna element is used the significant sidelobe is decreased to the level of about -16.50 dB (E - plane) and 14.21 dB (H-plane). Furthermore, it can be seen in Fig. 3 that the first sidelobes get lower from -15 dB for uniform case to -20 dB for exponential spacing scheme (E- plane) and from -16 dB for uniform case to -22 dB for exponential spacing scheme (H-plane). The backside lobe decreases from -21.15 dB (uniform spacing) to -38.26 dB (exponential spacing) for E-plane and from -22.37 dB (uniform spacing) to -39.51 dB (exponential spacing) for H-plane. At the same time, the beamwidth of the main beam increases from 4.77 deg (uniform spacing) to 7.22 deg (exponential spacing) for E-plane and from 4.44 deg (uniform spacing) to 7.04 deg (exponential spacing) for H-plane. Characteristics of other spacing schemes are shown in Tab. 4. to 9.

5.2.2 Antenna Elements Comprised by the Polynomial Function

The normalized radiation patterns of polynomial distributed antenna elements are given in Fig. 4. and show a significant reduction of sidelobe level. The results for this type of element spacing are very similar to the exponential spacing scheme.

5.2.3 Antenna Elements Comprised by the Trigonometrical Function

The trigonometrical spacing scheme results in a high decrease of the significant lobe level in comparison with the uniform spacing scheme. Also, the side lobe levels between -60 deg and +60 deg are equable. The normalized radiation pattern for the trigonometrical spacing scheme is shown in Fig. 5.

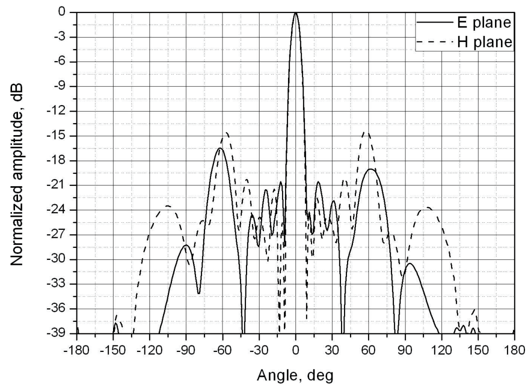

Fig. 3. Radiation pattern of nonuniformly distributed antenna elements (exponential function) placed on the sphere (E-plane and H-plane).

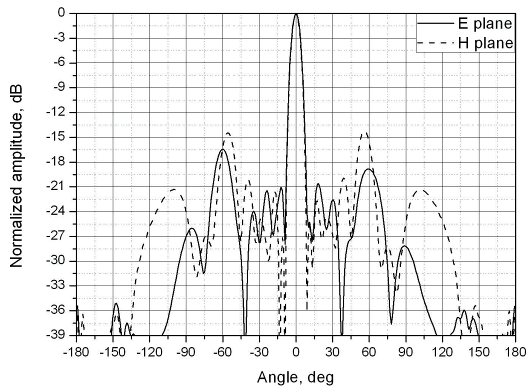

Fig. 4. Radiation pattern of nonuniformly distributed antenna elements (polynomial function) placed on the sphere (E-plane and H-plane).

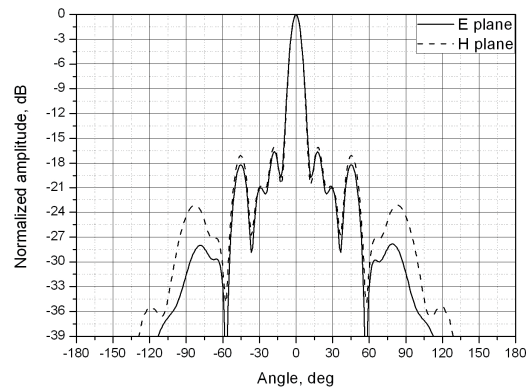

Fig. 5. Radiation pattern of nonuniformly distributed antenna elements (trigonometrical function) placed on the sphere (E-plane and H-plane).

5.2.4 Antenna Elements Comprised by the Logarithmic Function

This type of convex function for spacing of the elevation rings on the spherical surface results in the best values for significant sidelobe levels and beamwidth of the main beam. The side lobe levels between -60 deg and +60 deg are equable for both planes (E and H). The backside lobe decreases from -21 dB (uniform spacing) to -35.7 dB for E-plane and from -21.8 dB (uniform spacing) to -36 dB for H-plane.

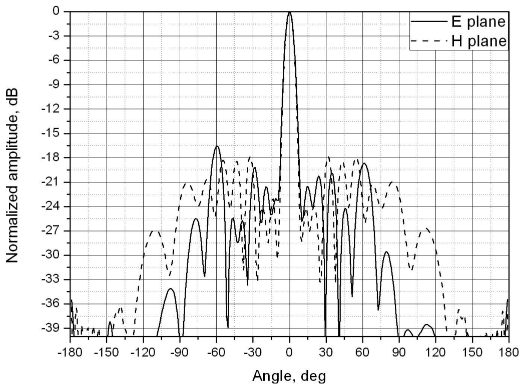

Fig. 6. Radiation pattern of nonuniformly distributed antenna elements (logarithmic function) placed on the sphere (E-plane and H-plane).

5.2.5 Antenna Elements Comprised by the Prime Number Spacing

This prime number array element was not spread out as rapidly as in other spacing schemes and the results are near the exponential and polynomial case. The normalized radiation pattern for prime number spacing scheme is shown in Fig. 7.

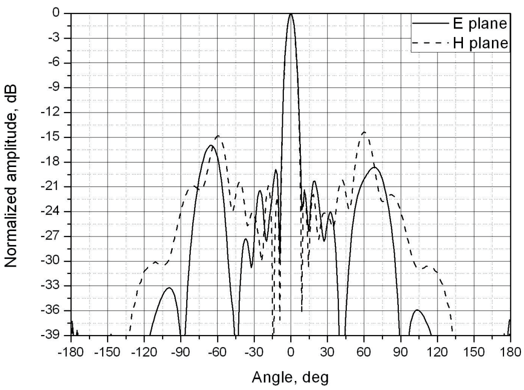

Fig. 7. Radiation pattern of nonuniformly distributed antenna elements (prime number spacing) placed on the sphere (E-plane and H-plane).

5.3 Summary

Increasing antenna elements (circular waveguide-fed aperture) density in convex manner results in:

- decreasing sidelobe levels;
- decreasing backside lobe levels;
- decreasing sidelobe levels in range abs(Angle)≥90^0;
- increasing beamwidth of the main beam (max. 1.8 beamwidth of uniform spacing scheme).

A summary comparison of radiation pattern characteristics of different convex spacing schemes is shown in Tab. 4, Tab. 5, Tab. 6 and Tab. 7.

If we compare characteristics of different spacing schemes it can be concluded that:

- logarithmic function results in maximum sidelobe level decrease (from -9.55 dB to -16.63 for E plane and from -12.66 dB to -17.79 dB for H plane);
- trigonometric function results in maximum backside lobe level decrease (from -21.15 dB to -40.08 for E plane and from -22.37 dB to -41.15 dB for H plane);
- polynomial function results in maximum side lobe level in range abs(Angle)≥90^0 decrease (from -26.21 dB to -35.16 for E plane);
- logarithmic function results in maximum side lobe level in range abs(Angle)≥90^0 decrease (from -19.99 dB to -30.08 for H plane) and
- logarithmic function results in minimum main beam beamwidth increase (from 4.78^0 to 6.20^0 for E plane and from 4.44^0 to 6.18^0 for H plane).

The data obtained demonstrate the possible advantages of using the nonuniform spacing scheme regarding the reduction of the sidelobe levels.

Tab. 4, 5, and 6 show a significant reduction of sidelobe levels when unequally spaced arrays are used, especially in relation to back lobes of uniform spaced arrays.

Fig.8. a) and b) show normalized radiation patterns of all the calculated elevational spacing schemes for E and H plane separately. As it can be seen, the first significant sidelobe level is the most supressed with nonuniform distribution for the case when logarithmic function for the embracing of the waveguides is used.

Tab. 8 and 9 show the spacing of the adjacent antenna element along circumference and the spacing of the adjacent rings along the sphere circumference. The adjacent rings and antenna element spacings of the nonuniform spacing schemes are generally lower than the uniform spacing scheme, except for the logarithmic function. So, antenna element density is higher for nonuniform spacing schemes.

Derivation of sets of distances by the logarithmic spacing scheme promises pattern improvement.

6. Conclusion

This paper presents spacing schemes for reducing sidelobe levels which could be easily calculated by computers. The amount of reduction of sidelobe level is quite significant. All antenna elements are fed equally and are progressively phased so that the field from all antenna elements could form appropriate main beam or radiation pattern. If arrays are arranged in this way, they have the ability to produce a desired radiation pattern and could satisfy requirements for many directive applications.

The numerical results show that the logarithmic array geometry provides the best results of reducing sidelobe by comparison with other array geometry, when uniformly spaced arrays is the reference kind of arranged arrays.

The use of unequal spacing is a possible method for reducing sidelobes but potentialities of nonuniformly spaced spherical antenna arrays have not been explored in detail yet.

	Uniform E, dB	Exponential E, dB	Polynomial E, dB	Trigonometric E, dB	Logarithmic E, dB	Prime number E, dB
E - plane	-9.55	-16.50	-16.39	-16.59	-16.63	-15.99
H - plane	-12.66	-14.21	-14.21	-16.05	-17.79	-14.29

Tab. 4. First significant sidelobe level for different array geometry.

	Uniform	Exponential	Polynomial	Trigonometric	Logarithmic	Prime number
	E, dB	E, dB	E, dB	E, dB	E, dB	E, dB
E - plane	-21.15	-38.26	-35.42	-40.08	-35.50	-37.29
H - plane	-22.37	-39.51	-36.60	-41.15	-36.42	-38.15

Tab. 5. Backside lobe level for different array geometry.

	Uniform	Exponential	Polynomial	Trigonometric	Logarithmic	Prime number
	E, dB	E, dB	E, dB	E, dB	E, dB	E, dB
E - plane	-26.21	-28.26	-35.16	-27.90	-34.13	-33.10
H - plane	-19.99	-23.46	-21.28	-24.09	-26.65	-30.08

Tab. 6. Highest side lobe level in range ***abs*(Angle)** $\geq 90^0$ for different array geometry.

	Uniform	Exponential	Polynomial	Trigonometric	Logarithmic	Prime number
	HPBW (deg)	HPBW (deg)	HPBW (deg)	HPBW (deg)	HPBW (deg)	HPBW (deg)
E - plane	4.78	7.22	7.10	8.53	6.20	7.28
H - plane	4.44	7.04	6.90	5.98	6.18	7.14

Tab. 7. Beamwidth of the main beam for different array geometry.

$d_{lk} = \dfrac{2\pi\, r_s \sin\alpha_l}{N_l}$, [22]	Uniform	Exponential	Polynomial	Trigonometric	Logarithmic	Prime number
Min. spacing d_{lk}/λ_0	1.67 ($l = 2$)	0.88 ($l = 5$)	0.88 ($l = 5$)	0.88 ($l = 5$)	0.88 ($l = 5$)	0.93 ($l = 5$)
Max. spacing d_{lk}/λ_0	1.99 ($l = 5$)	1.29 ($l = 1$)	1.60 ($l = 1$)	1.46 ($l = 1$)	1.60 ($l = 1$)	1.26 ($l = 1$)

Tab. 8. The spacing of the adjacent antenna element along circumference (here N_l is the number of antenna elements distributed on the l^{th} ring).

$d_{l-1,l} = \dfrac{\pi\, r_s(\alpha_{l-1} - \alpha_l)}{180}$	Uniform	Exponential	Polynomial	Trigonometric	Logarithmic	Prime number
Min. spacing $d_{l-1,l}/\lambda_0$	1.61 (*all*)	0.70 (d_{56})	0.70 (d_{56})	0.70 (d_{56})	0.70 (d_{56})	0.74 (d_{56})
Max. spacing $d_{l-1,l}/\lambda_0$	1.61 (*all*)	1.13 (d_{12})	1.19 (d_{12})	1.18 (d_{12})	2.04 (d_{12})	0.99 (d_{12})

Tab. 9. The spacing of the adjacent rings along the sphere circumference.

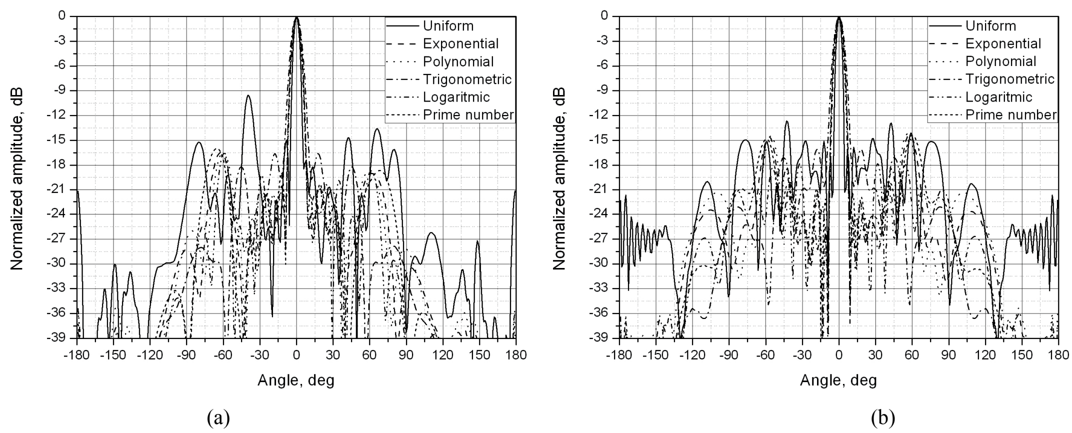

Fig. 8. Radiation pattern of uniformly distributed antenna elements in comparison with radiation pattern of nonuniformly distributed antenna elements placed on the sphere for: a) E-plane, b) H-plane.

Acknowledgements

This work has been sponsored and supported by the Croatian Inst. of Technology (TEST program) under contract between the Croatian Inst. of Technology, Faculty of Electrical Engineering Univ. of Osijek and Svijet racunala d.o.o. Osijek.

References

[1] MOLISCH, A.-F. *Wireless Communication*. John Wiley & Sons, LTD, IEEE Communication Society, 2005.

[2] UNZ, H. Linear arrays with arbitrarily distributed elements. I*RE Transactions on Antennas and Propagation*, March 1960, vol. AP-8, p. 222 - 223.

[3] KING, D. D., PACKARD, R. F., THOMAS, R. K. Unequally spaced, broad-band antenna arrays. *IRE Transactions on Antennas and Propagation,* July 1960, vol. AP-8, p. 380 - 385.

[4] SANDLER, S. S. Some equivalence between equally and nonequally spaced arrays. *IRE Transactions on Antennas and Propagation*, March 1961, vol. AP-9, p. 496-500.

[5] HARRINGTON, R.-F. Sidelobe reduction by nonuniform element spacing. *IRE Transactions on Antennas and Propagation*, March 1961, p. 187 - 192.

[6] ANDREASEN, M. G. Linear arrays with variable interelement spacing. *IRE Transactions on Antennas and Propagation*, March 1962, vol. AP-10, p. 137 - 143.

[7] ISHIMARU, A. Theory of unequally-spaced arrays. I*RE Transactions on Antennas and Propagation*, November 1962, vol. AP-8, p. 691 - 702.

[8] HODJAT, F., HOVANESSIAN, A. A. Nonuniformly spaced linear and planar array antennas for sidelobe reduction. I*EEE Transactions on Antennas and Propagation*, March 1978, vol. AP-26, no. 2, p. 198 - 204.

[9] JARSKE, P., SARAMAKI, T., MITRA, S. K., NEUYO, Y. On properties and design of nonuniformly spaced linear arrays. *IEEE Transactions on Acoustics, Speech and Signal Processing*, March 1988, vol. 36, no. 3, p. 372 - 380.

[10] POZAR, D. M., KAUFMAN, B. Design considerations for low sidelobe microstrip arrays. *IEEE Transactions on Antennas and Propagation*, August 1990, vol. 38, no. 8, p. 1176 – 1185.

[11] JEFFERS, J. L., BOUCHER, S. G. Optimum unequally spaced arrays and their amplitude shading. In *Proceedings of Ultrasonics Symposium*, November 1995, vol. 2, p. 965 - 969.

[12] KUMMAR, B. P., BRANNER, G. R. Generalized analytical technique for the synthesis of unequally spaced arrays with linear, planar, cylindrical or spherical geometry. *IEEE Transactions on Antennas and Propagation*, February 2005, vol. 53, no. 2, p. 621-634.

[13] SHIHAB, M., NAJJAR, Y., DIB, N., KHODIER, M. Design of non-uniform circular antenna array using Particle Swarm Optimization. *Journal of Electrical Engineering*, 2008, vol. 59, no. 4, p. 216 – 220.

[14] ABDOLEE, R., VAKILIAN, V., RAHMAN, T. A. Elements space and amplitude perturbation using Genetic Algorithm for antenna sidelobe cancellation. *Signal Processing: An International Journal* (*SPIJ*), March/April 2008, vol. 2, no. 2, p. 10 – 16.

[15] BEVELAQUA, P. J., BALANIS, C. A. Geometry and weight optimization for minimizing sidelobes in wideband planar arrays. *IEEE Transactions on Antennas and Propagation*, April 2009, vol. 57, no. 4, p. 1285 – 1289.

[16] TAM, W. T., LUK, K. M. Resonance in spherical-circular microstrip structures. *IEEE Transactions on Microwave Theory and Technique*, April 1991, vol. MTT-39, p. 700 - 704.

[17] LEIJON, R. Radiation from mobile phone antennas close to the human body. *Technical Report No. 270L*, Dept. of Microwave Technology, Chalmers Univ. of Technology, Gothenburg, Aug. 1997.

[18] RUPCIC, S., MANDRIC, V., RIMAC-DRLJE, S. Fabrication errors influence on the spherical array radiation pattern. *Radioengineering*, September 2010, vol. 19, no. 3, p. 378 – 385.

[19] SIPUS, Z., KILDAL, P.-S., LEIJON, R., JOHANSSON, M. An algorithm for calculating Green's functions for planar, circular cylindrical and spherical multilayer substrates. *Applied Computational Electromagnetics Society Journal*, 1998, vol. 13, p. 243 – 254.

[20] SENGUPTA, D. L., SMITH, T. M., LARSON, R. W. Radiation characteristics of spherical array of circularly polarized elements. *IEEE Trans. on Antennas and Propagation*, 1968, vol. 16, p. 2 – 7.

About Authors ...

Slavko RUPCIC received his B.Sc. degree in Electrical Engineering from the University of Split, Faculty of Electrical Engineering, Mechanical Engineering and Naval Architecture, in 1989. He received his M.Sc. and Ph.D. degree in Electrical Engineering from the University of Zagreb, Faculty of Electrical Engineering and Computing, in 1994 and 2009, respectively. Since 1990 he has worked at the Faculty of Electrical Engineering, University of Osijek at the Dept. of Communications - Laboratory for HF measurements. In recent years, he has been involved in different research activities including measurement, modeling and simulation of different radiating structures on conformal surfaces. His research interests include antenna analysis, numerical computation of radiating structures and radio communications systems. He is a member of IEEE, Antenna and Propagation Society.

Vanja MANDRIC received her B.Sc. degree in Electrical Engineering from J. J. Strossmayer University of Osijek in 2005. Since 2005 she has been an assistant at the Faculty of Electrical Engineering, University of Osijek, Dept. of Communications, Laboratory for HF measurements. Her research interests include areas of antenna analysis, numerical computation of radiating structures and radio communications systems.

Drago ZAGAR received the B.Sc., M.Sc. and Ph.D. from the University of Zagreb, Faculty of Electrical Engineering and Computing, in 1990, 1995, 2002, respectively. From the 1990 he was affiliated with the Dept. of Communications, Faculty of Electrical Engineering, University of Osijek, where he has reached a rank of associate professor. From 2003 to 2005 he was the Vice-Dean for education, and currently he is the Vice-Rector for education and students at the University of Osijek. His main research interests include Quality of Service in IP networks, formal methods for protocol verification, and computer networks. He has served in technical program committees of several conferences. He is a member of IEEE (Communication Society) and ACM.